New Phytologist

Differences in grapevine rootstock sensitivity and recovery from drought are linked to fine root cortical lacunae and root tip function

Italo F. Cuneo[1], Felipe Barrios-Masias[2], Thorsten Knipfer[3], Jake Uretsky[3], Clarissa Reyes[3], Pierre Lenain[3], Craig R. Brodersen[4], M. Andrew Walker[3] and Andrew J. McElrone[3,5]

[1]Department of Agriculture and Food Sciences, Pontificia Universidad Católica de Valparaíso, Valparaíso 2340025, Chile; [2]Department of Agriculture, Veterinary and Rangeland Sciences, University of Nevada, Reno, Reno, NV 89557, USA; [3]Department of Viticulture and Enology, University of California, Davis, CA 95618, USA; [4]School of Forestry and Environmental Studies, Yale University, New Haven, CT 06511, USA; [5]Crops Pathology and Genetics Research Unit, USDA-ARS, Davis, CA 95618, USA

Authors for correspondence:
Andrew J. McElrone
Tel: +1 530 754 9763
Email: ajmcelrone@ucdavis.edu

Italo F. Cuneo
Tel: +56 32 2372913
Email: italo.cuneo@pucv.cl

Received: *23 December 2019*
Accepted: *5 March 2020*

New Phytologist (2021) **229:** 272–283
doi: 10.1111/nph.16542

Key words: cortical lacunae, drought stress, Lp_r, recovery, root growth, suberin deposition.

Summary

- Structural changes during severe drought stress greatly modify the hydraulic properties of fine roots. Yet, the physiological basis behind the restoration of fine root water uptake capacity during water recovery remains unknown.
- Using neutron radiography (NR), X-ray micro-computed tomography (micro-CT), fluorescence microscopy, and fine root hydraulic conductivity measurements (Lp_r), we examined how drought-induced changes in anatomy and hydraulic properties of contrasting grapevine rootstocks are coupled with fine root growth dynamics during drought and return of soil moisture.
- Lacunae formation in drought-stressed fine roots was associated with a significant decrease in fine root Lp_r for both rootstocks. However, lacunae formation occurred under milder stress in the drought-resistant rootstock, 110R. Suberin was deposited at an earlier developmental stage in fine roots of 101-14Mgt (i.e. drought susceptible), probably limiting cortical lacunae formation during mild stress. During recovery, we found that only 110R fine roots showed rapid re-establishment of elongation and water uptake capacity and we found that soil water status surrounding root tips differed between rootstocks as imaged with NR.
- These data suggest that drought resistance in grapevine rootstocks is associated with rapid re-establishment of growth and Lp_r near the root tip upon re-watering by limiting competing sites along the root cylinder.

Introduction

Root systems of woody perennial plants, like grapevine, are generally described as having permanent, suberized coarse roots and fine roots that are either suberized or unsuberized (Kramer & Boyer, 1995; Keller, 2010; Comas *et al.*, 2013). The suberization process involves lignin and suberin deposition in the cell wall matrix (Geldner, 2013). While they constitute as little as 1% of the total root surface area for many woody species (Kramer & Bullock, 1966), unsuberized fine roots are the primary exchange surface between woody plants and soil, accounting for the vast majority of water absorption (Kramer & Bullock, 1966; Kramer & Boyer, 1995; Gambetta *et al.*, 2013) and mediate plant–soil hydraulic redistribution (Richards & Caldwell, 1987). Traditionally, fine roots have been defined as all roots ≤ 2 mm in diameter, yet it is now recognized that this approach does not capture the diversity of form and function observed among fine root orders (McCormack *et al.*, 2015), nor does it account for stress-induced shifts in root function. Targeting the underlying root system anatomy and physiology of the functional fine roots related to successful water uptake should then allow for a deeper understanding of resistance during periods of stress.

Water absorbed by fine roots must traverse several cell layers in the radial pathway before reaching the stele (Steudle & Peterson, 1998). Along this path, transport of water can occur through a combination of apoplastic (i.e. outside the plasma membrane and in the cell walls and intercellular spaces), symplastic (i.e. continuum of cytoplasm interconnected by plasmodesmata and excluding vacuoles) and transcellular (i.e. crossing membranes) pathways (Steudle & Peterson, 1998; Steudle, 2000). At the endodermis, the apoplastic pathway is blocked by a gasket-like band of suberin named the 'Casparian strip', a hydrophobic barrier that inhibits the route of water in the apoplast. This band forces water to cross via the cell to cell pathway (i.e. either symplastic or transmembrane). The radial hydraulic properties of *Vitis* fine roots change with the developmental stage (i.e. meristematic : elongation, maturation and secondary growth zones), in response to the formation of

suberized apoplastic barriers at the exodermis and endodermis and by regulation of aquaporins (Maurel *et al.*, 2008; Vandeleur *et al.*, 2009; Gambetta *et al.*, 2013). In a recent study, the radial pathway from the soil–root interface to the xylem was reported to constitute 81% of the whole-plant hydraulic resistance in well watered olive plants and up to >95% in plants under moderate water stress, pointing out the importance of this hydraulic pathway in whole-plant functionality (Rodriguez-Dominguez & Brodribb, 2020).

Under drought, root systems are challenged to absorb adequate soil water to meet the transpiration demands of the canopy. Roots are hypothesized to operate like electrical fuses that disconnect when carrying an excessive load under drought (Zimmermann, 1983; Jackson *et al.*, 2000). The exact sites and sequence of anatomical, biochemical, and physiological events leading to root dysfunction remain largely elusive despite advances over the last few decades on drought response of roots (Aroca *et al.*, 2011; Barrios-Masias *et al.*, 2015; van Dusschoten *et al.*, 2016). For example, lignin–suberin deposition in the root endodermis, which increases the hydraulic resistance of the apoplast, was reported to differ between grapevine rootstock cultivars during prolonged drought cycles (i.e. 15–20 d; Barrios-Masias *et al.*, 2015). Furthermore, lacunae formation during mild drought stress (i.e. −0.6 MPa Ψ_{stem}, single drought cycle) and root shrinkage due to the collapse of root cortex tissue during severe drought stress have been reported to greatly modify the internal structure and hydraulic properties of unsuberized fine roots (North & Nobel, 1991; Cuneo *et al.*, 2016). It is not known how lacunae formation, suberin–lignin deposition and fine root growth dynamics coincide to impact the hydraulic capacity of a damaged fine root upon re-watering after drought. Previous studies using neutron radiography (NR) have also concluded that rhizosphere hydrophobicity can limit root water uptake after drying and subsequent rewetting (Ahmed *et al.*, 2015; Benard *et al.*, 2015; Zarebanadkouki *et al.*, 2018). These responses were dependent on the position along the length of the root cylinder (i.e. Carminati, 2013), and rhizosphere hydrophobicity occurs mainly in older and proximal root sections, while young root segments maintain their hydraulic connection with the surrounding soil (Carminati, 2013). Further experiments are needed to evaluate whether this pattern holds for different types of roots and species, and how it integrates with other responses described above.

In this study, we used grapevine rootstocks 110R (*V. berlandieri* × *V. rupestris*), considered drought resistant, and 101-14Mgt (*V. riparia* × *V. rupestris*), considered drought susceptible (Pongrácz, 1983; Christensen, 2003) to study how drought-induced cortical lacunae formation, suberin–lignin deposition and root growth dynamics are coupled with water uptake capacity during and after drought. We hypothesized that, in the drought-resistant rootstock, as distinct from the drought-susceptible one, structural changes during drought shifts water uptake patterns along the length of roots, helping to ensure adequate water supply to the growing root tip; this would rapidly re-establish growth and water uptake capacity during water recovery. To test this, we used NR, X-ray micro-computed tomography (micro-CT), fluorescence microscopy and hydraulic measurements on fine roots.

Materials and Methods

Plant material and growing conditions

Plants of Millardet et de Grasset 101-14 (101-14Mgt; *V. riparia* × *V. rupestris*) and Richter 110 (110R; *V. berlandieri* × *V. rupestris*) were propagated from herbaceous cuttings collected from parent plants in the University of California, Davis, USA vineyards. The basal node of each cutting was soaked in 2.5% rooting solution (Earth Science Products, Wilsonville, Oregon, USA), placed in a plastic tray filled with perlite, and maintained in a fog room for *c.* 15 d until root initiation and growth (Knipfer *et al.*, 2015). For the neutron radiography experiment (NR), cuttings were transplanted into aluminum containers of 31 cm length, 31 cm width and 1.9 cm depth. For the micro-CT, root hydraulics and fluorescence microscopy experiments, plants were grown in 1.1 l plastic pots filled with the same sand. Plant growth was maintained under glasshouse conditions (*c.* 25°C to 30°C temperature, 35% relative humidity, 1000–1500 µmol photons $m^{-2} s^{-1}$, and 16 : 8 h, light : dark cycle), and watered twice a day with water supplemented with macronutrients and micronutrients (similar to Gambetta *et al.*, 2013). Water stress was induced by stopping irrigation. At the point of measurement, plants had one or two shoots of *c.* 30 cm in length with eight to 12 leaves. In this work, fine roots analyzed were branched clusters of absorptive roots of first, second and third order (McCormack *et al.*, 2015).

Measurements of plant water status

A Scholander pressure chamber (Soil Moisture Equipment Corp. 3005, Goleta, CA, USA) was used to measure stem water potential (Ψ_{stem}) of plants in the NR and micro-CT experiments. Mature leaves were placed into Mylar covered plastic bags for at least 15 min, such that they were hydraulically equilibrated with stem xylem. Subsequently, leaves were excised at the base of the petiole and placed into the pressure chamber, while still bagged. The chamber was pressurized, and the balancing pressure required to force water out of the petiole base was recorded and defined as Ψ_{stem}. Stress levels were defined based on previous results (Cuneo *et al.*, 2016), where the threshold for cortical lacunae formation was *c.* −0.6 MPa. Here we defined stress levels as well watered (≥ −0.6 MPa Ψ_{stem}), mild stress (between −0.6 MPa and −1.4 Ψ_{stem}), severe stress (≤ −1.4 MPa Ψ_{stem}) and recovery after re-watering (≥ −0.6 MPa Ψ_{stem}).

Neutron radiography

To study the growth and water uptake by fine roots during the drought experiments we used *in vivo* NR imaging. These observations were performed at the 2-megawatt Training, Research, and Isotope Production and General Atomics reactor at McClellan Nuclear Research Center (MNRC; http://mnrc.ucdavis.edu), Bay 3. Plants were grown in sand-filled aluminum containers that are effectively transparent to neutrons, while hydrogen in the soil and plant water are attenuated strongly (Pleinert & Lehmann,

1997; Menon *et al.*, 2007). The neutron beam has a length to diameter ratio of 140, which yields an image of 2048 × 2048 pixels with a spatial resolution of 0.169 mm per pixel that is captured with a charge coupled device (CCD) camera detector. Plants that were established in the aluminum containers were transported from the UC Davis growth chamber facility to the MNRC and Ψ_{stem} was measured immediately upon arriving. The aluminum containers then were mounted in the MNRC neutron beamline (see Supporting Information Fig. S1) where they were scanned every *c.* 2–3 d to track root elongation dynamics and water uptake before, during and after drought stress. Ψ_{stem} was measured before every scanning time. In order to estimate root growth under well watered conditions, a scan was taken 1 d before the dry-down was initiated (i.e. day 0). During the dry-down, which occurred over *c.* 1 wk, plants remained at the MNRC facility under similar growth conditions using supplemental lighting. Ψ_{stem} was used to classify drought stress categories as: well watered, mild and severely stressed and re-watered.

Radiograph images were processed using Fiji imaging-processing software (ImageJ; www.fiji.sc; Schindelin *et al.*, 2012) as follows: (1) radiographs were de-speckled to reduce noise; (2) radiographs of different days for the same container were stacked; (3) the whole image stack for each container was cropped in a rectangular shape containing five root tips; (4) the Trainable Weka Segmentation plug-in was used to classify roots in the stack; (5) the 'make binary' and 'skeletonize' functions were applied followed by a convolve filter (matrix = [1515255151]); and (6) the stack was analyzed with the histogram function. The analyzed roots were distributed in depth and laterally in order to avoid possible errors related to soil moisture heterogeneity. Water depletion in the soil surrounding the maturation root zone was calculated using gray value intensities (lower in wetter portions of the image and higher as soil moisture is depleted). First, a line of 70 pixels (i.e. 11.8 mm) was drawn across the fine root portion (i.e. between root tip and maturation zone; 11.8 mm from the distal part of the root tip; Gambetta *et al.*, 2013), covering also the surrounding soil. Then, the 'plot profile' function was applied in order to obtain gray value intensities for the distance of the line drawn (Fig. S2). Then, a slope was calculated using the gray value intensities of the surrounding soil.

X-ray micro-CT

X-ray imaging of plant tissue was performed at the Advanced Light Source (ALS) Lawrence Berkeley National Laboratory, beamline 8.3.2, to study drought-induced structural changes in grapevine fine roots. Plants were transported by car from the UC Davis campus to ALS. Upon arriving, Ψ_{stem} was measured immediately. The root systems were carefully removed from the pots, and fine roots were excised at *c.* 10 cm from the tip. Each root was wrapped in wax tape (Parafilm M®, Bemis Co., Neenah, WI, USA) containing petroleum jelly in the interior to prevent desiccation. Our previous work confirmed that excision in this manner did not alter the status of the tissue (Cuneo *et al.*, 2016). The wrapped roots were mounted into a drill chuck, fixed on an air-bearing stage (Brodersen *et al.*, 2010; McElrone *et al.*, 2013; Knipfer *et al.*, 2015; Cuneo *et al.*, 2016) and imaged using an 18 keV synchrotron X-ray beam. Roots were imaged targeting the maturation region where mature xylem start to appear (Gambetta *et al.*, 2013). During the scanning, 1024 longitudinal images were taken in 180° rotation and 200 s exposure time. Images were collected using a 4008 × 2672-pixel CCD camera (#PCO 4000; Cooke Corp., Eliot, ME, USA). The resolution of the images was 1.8 µm per pixel. The acquired images were reconstructed into a stack of transverse images using Octopus 8.3 software (Institute for Nuclear Sciences, Ghent University, Ghent, Belgium), a custom plug-in for Fiji imaging-processing software (ImageJ).

Fluorol yellow 088 staining

To determine the degree of suberization of the roots we made free-hand cross-sections of roots with razor blades targeting two developmental regions (i.e. maturation and secondary growth). Roots were then stained with 0.1% (w/v) Fluorol Yellow (Fluorol yellow 088; Santa Cruz Biotechnology, Dallas, TC, USA) for 1 h and rinsed with tap water. The stained sections were mounted on a slide with diH_2O and observed under violet fluorescence light (excitation filter, 450–490 nm; dichromatic mirror, 495 nm; and emission filter, 525 nm) using a Leica DM4000 B LED compound microscope (Leica Microsystems, Buffalo Grove, IL, USA). Images were acquired with a Leica DFC7000 digital camera. With this method, suberin in the exodermis and endodermis appeared bright yellow (Brundrett *et al.*, 1991).

Hydraulic properties of fine roots

The root hydraulic conductivity (Lp_r) was measured for plants under well watered conditions, under drought across a gradient of Ψ_{stem}, and after recovery from drought. Once transported to the laboratory, the whole root system was carefully removed from the pot under water to prevent damage to the roots. The root system was placed in another bucket with water, so it was easier to select the roots and three fine roots were excised under water at *c.* 10 cm from the tip. Lp_r was measured osmotically to prevent the collapsing of cortical lacunae (Cuneo *et al.*, 2016), as would be the case by pressurizing the root to obtain a hydrostatic Lp_r. To track the flow, we used a glass microcapillary (0.25-mm i.d.; Stoelting) connected to the end of the root and the connection was sealed with superglue (Loctite 409 gel; Henkel, Düsseldorf, Germany). The microcapillary was half-filled with diH_2O, and the roots were immersed in sucrose solutions of 0, 0.17, and 0.30 MPa. The osmotic pressure steps were applied in a descending order, and the displacement of the meniscus was tracked every 5 min. The 0.30 MPa osmotic pressure step was applied twice to check how flow was compared with the initial measurement, and roots were rinsed with diH_2O in between each pressure step. The volume (V) for each pressure step was obtained using the equation:

$$V = \pi(r^2)d,$$

where r is the radius of the microcapillary and d corresponds to the distance traveled by the meniscus. Because water flow

directionality was different depending on the osmotic pressure step (i.e. inward flow for 0 MPa and outward flow for 0.3 MPa), a negative sign (−) was assigned to volumes with outward directionality and a positive (+) was assigned to volumes with inward directionality. Then, volumetric flow rate (Q; $m^3\,s^{-1}$) was calculated as the slope of the linear regression line between the cumulative volume (m^3) and cumulative time (s). A second linear regression line was fitted between Q and the osmotic pressure gradient (ΔP), and the slope of this line represented hydraulic conductance (K; $m^3\,s^{-1}\,MPa^{-1}$; see Fig. S3). The surface area (A; m^2) of the root was measured using WINRHIZO (Régent Instruments, Ville de Québec, Canada), and Lp_r ($m\,s^{-1}\,MPa^{-1}$) was calculated using the equation:

$$Lp_r = K/A.$$

Statistical analysis

ANOVA and *t*-tests were performed using R v.3.3.2 statistical computing environment (R Core Team, 2016) with aid from the CAR software package (Fox & Weisberg, 2011). When appropriate, the Shapiro–Wilk test and Levene's test were used to test the assumptions of normality of residuals and homogeneity of variances, respectively. Data were transformed as necessary when assumptions were not met.

Results

Neutron radiography

We used NR imaging for *in vivo* visualization of fine root elongation dynamics in the drought-resistant and drought-susceptible rootstock during drought stress and recovery after 2 d of re-watering (see Figs 1a,b, S4). During the dry-down (i.e. from well watered to severe stress level), root elongation ($mm\,d^{-1}$) was reduced *c.* 30% for both rootstocks with increasing stress (i.e. more negative Ψ_{stem}; Fig. 1c). Both rootstocks maintained active root elongation during mild drought stress and responded similarly to different levels of drought stress (i.e. dry-down), displaying similar values of Ψ_{stem} (Fig. 1c). However, during the recovery period (i.e. after 2 d of re-watering), root elongation of the drought-resistant rootstock (110R) recovered rapidly and approached rates comparable with the well watered plants that had not undergone the drought treatment. Conversely, the drought-susceptible rootstock (101-14Mgt) did not recover root elongation rates in the same time frame, and root elongation rates

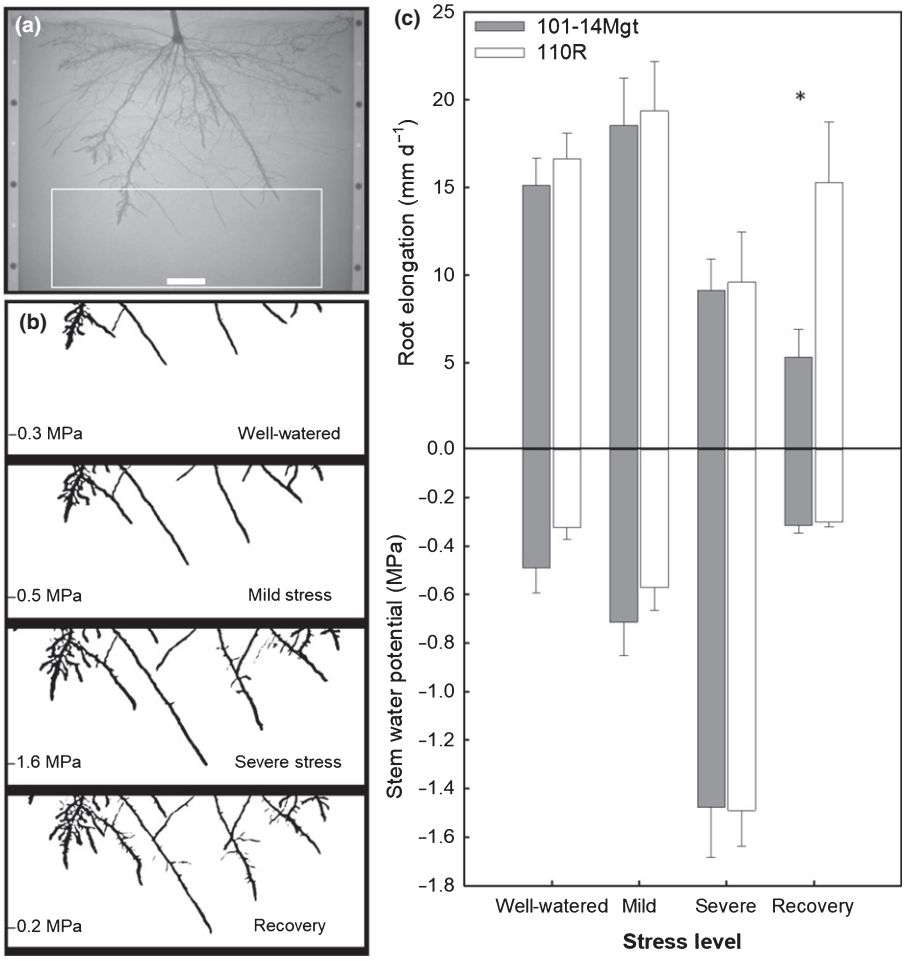

Fig. 1 Neutron radiography was used to track root elongation dynamics during drought in grapevine rootstocks. (a) Representative example of a neutron radiograph from 101-14Mgt rootstock. The white box denotes the region where root tips were tracked. (b) Correspond to the cropped region of radiograph in (a), after image processing and for different stress levels (i.e. well watered, mild, severe and recovery). (c, upper panel) Root elongation ($mm\,d^{-1}$) of 101-14Mgt and 110R rootstocks from data collected using the process described in (b). (c, lower panel), Stem water potentials observed for 101-14Mgt and 110R rootstocks at each stress level. Data are mean ± SE ($n = 7$). Asterisks indicate significant differences between rootstocks at each stress level as determined by *t*-test. *, $P < 0.05$. Bar in (a), 3.2 cm.

were even lower during the recovery period than for severely drought-stressed plants (Fig. 1c; $P = 0.018$).

X-ray microtomography imaging and fluorescence microscopy

We used X-ray microtomography (micro-CT) imaging to visualize cortical lacunae formation in fine roots under well watered, mild and severe drought conditions for each rootstock (i.e. Ψ_{stem} as described above). In well watered plants, there was no evidence of cortical lacunae in either rootstock, yet cortical lacunae tended to form at different stress levels for the rootstocks studied (Fig. 2a,b). The analysis of percentage of lacunae in the cortex showed that cortical lacunae tended to form earlier during stress in the drought-resistant rootstock (i.e. mild drought stress) than in drought-susceptible one (i.e. severe drought stress; see Figs 2a,

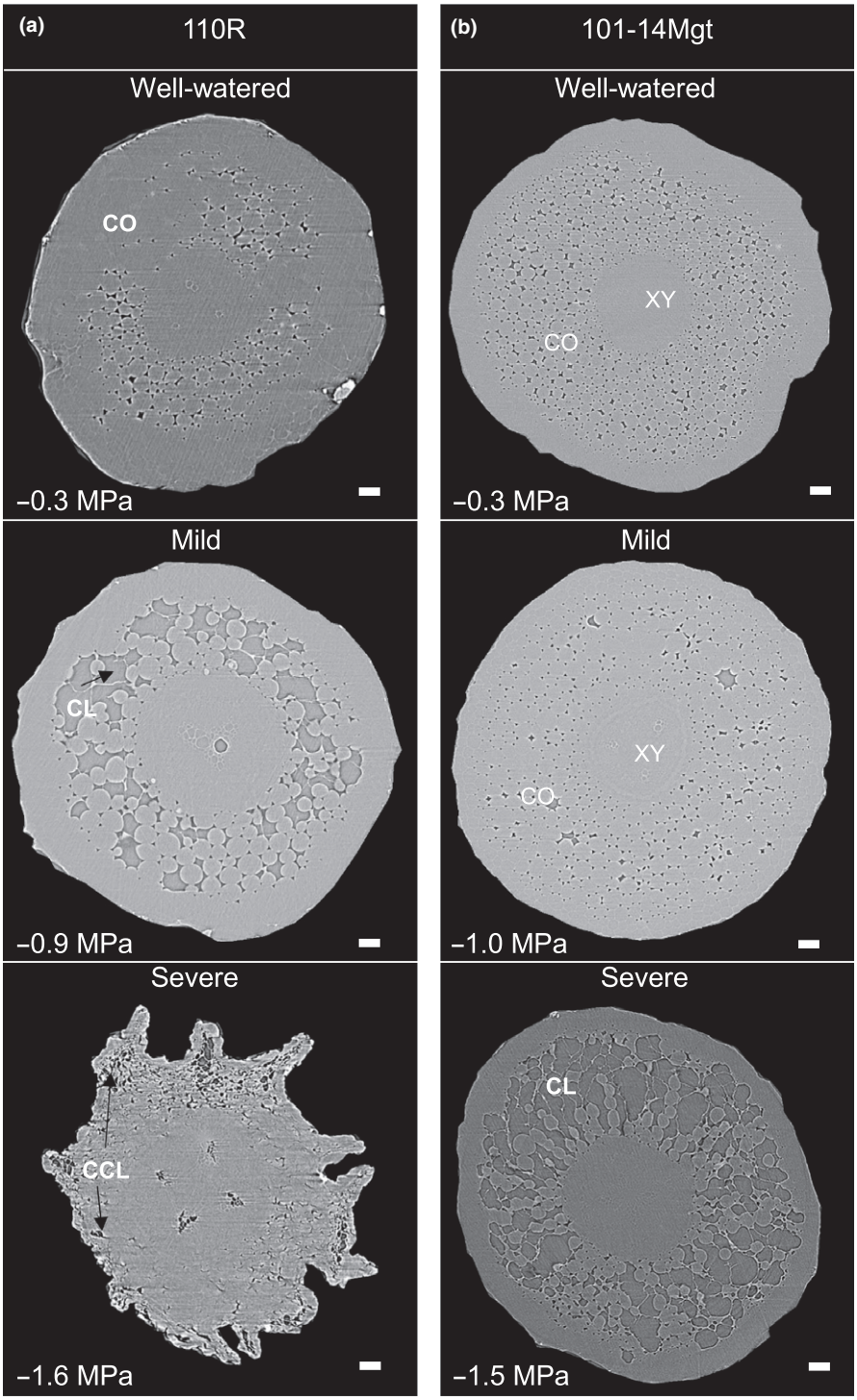

Fig. 2 Representative slices from micro-CT showing anatomical traits of grapevine fine roots under well watered (≥ −0.6 MPa Ψ_{stem}), mild drought stress (i.e. *c.* between −0.6 MPa and −1.4 Ψ_{stem}), and severe drought stress (≤ −1.4 MPa Ψ_{stem}) for 110R in (a) and 101-14Mgt in (b). Micro-CT revealed lacunae formation in 110R (a) fine roots under mild drought stress (indicated with a black arrow); something that happened during severe drought stress 101-14Mgt. Collapsed cortical lacunae and root shrinkage is visible during severe drought stress in 110R (indicated with black arrows). CCL, collapsed cortical lacunae; CL, cortical lacunae; CO, cortex; XY, xylem. Bars, 200 μm.

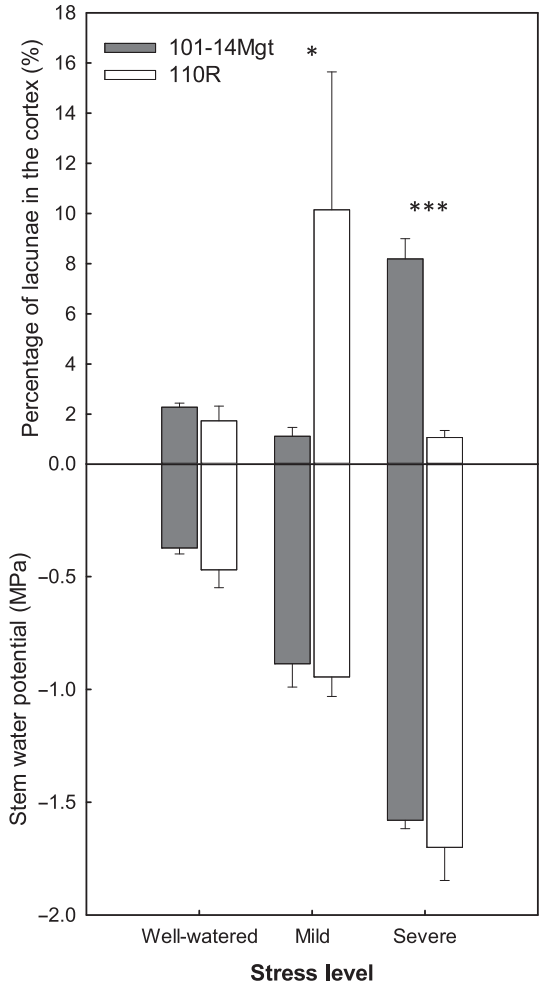

Fig. 3 Percentage of lacunae in the cortex and stem water potentials observed at different stress levels (i.e. well watered, mild and severe) for 101-14Mgt and 110R grapevine rootstocks. Data are mean ± SE ($n = 15$). Asterisks indicate significant differences between rootstocks at each stress level as determined by *t*-test. *, $P < 0.05$; ***, $P < 0.001$.

b, 3). Also, cortical lacunae tended to collapse in the drought-resistant rootstock during severe drought stress (see Fig. S2a), yielding less percentage in cortical lacunae compared to the drought-susceptible one at this stress level (Fig. 3). Significant differences of percentage of lacunae in the cortex were found at mild ($P = 0.046$) and severe drought stress ($P = 0.0001$) when comparing rootstocks, while no differences of Ψ_{stem} between the rootstocks were found at each stress level (Fig. 3).

Fluorescence microscopy was used to visualize suberin deposition in two developmental regions of fine roots (i.e. maturation and secondary growth) under well watered and mild drought conditions for each rootstock (i.e. Ψ_{stem} as described above). In the maturation region, no suberin deposition was found in the exodermis and endodermis of 110R, the drought-resistant rootstock, under well watered and drought conditions, while suberin deposition in plants experiencing drought was visible in the exodermis of the drought-susceptible one (Fig. 4). In the secondary growth region, the drought-susceptible rootstock (101-14Mgt) showed a regular suberin deposition in the exodermis and endodermis under well watered and drought conditions (Fig. 4). In this developmental region, the drought-resistant rootstock (110R) showed suberin deposition in the endodermis, but the exodermis remain unsuberized under well watered and drought conditions (Fig. 4).

Drought effects on root hydraulic conductivity

Under well watered conditions, no differences in Lp_r were found between the rootstocks (Fig. 5). We observed a reduction of *c.* 45% in Lp_r in the drought-resistant rootstock but no reduction in Lp_r for the drought-susceptible one during mild drought stress (Fig. 5; $P = 0.0012$). During severe drought stress, the drought-susceptible rootstock showed pronounced reduction in Lp_r (i.e. *c.* 73% of reduction compared with well watered plants), while the Lp_r of the drought-resistant rootstock decreased to *c.* 58% compared with well watered plants (Fig. 5). During recovery (i.e. plants that were re-watered for 2 d after reaching *c.* −1.7 MPa Ψ_{stem}), Lp_r of the drought-resistant rootstock was significantly higher (i.e. recovery to *c.* 68% of well watered plants; $P = 0.0001$) than the drought-susceptible rootstock that displayed an even lower Lp_r than that observed during severe drought stress (see Fig. 5). Ψ_{stem} of both rootstocks recovered completely to values similar to those shown in well watered plants (Fig. 5).

Assessment of root–soil interface with neutron radiography

To evaluate the soil immediately adjacent to fine roots tips (i.e. 11.8 mm back from the root apex) during well watered, severe drought and after 2 d of re-watering conditions, water status slopes were measured using a profile of gray value intensities (see Figs 6a,b, S2). The mean slope of water status in the region surrounding root tips did not differ between rootstocks during well watered and severe drought conditions (Fig. 6c). Yet, the mean slope of water status of the surrounding soil of root tips was significantly higher in the drought-resistant rootstock (1.42) compared with the drought-susceptible one (0.22; Fig. 6c; $P = 0.0001$).

Discussion

In this study, root physiological and anatomical parameters were studied together to better understand drought resistance in two contrasting grapevine rootstocks, 101-14Mgt (drought susceptible) and 110R (drought resistant). *In vivo* NR imaging showed no difference between rootstocks in root tip elongation rates during well watered and drought conditions. However, root tip elongation rates showed rapid recovery in 110R, the drought-resistant rootstock, after re-watering, while in 101-14Mgt, the drought-susceptible rootstock, this rate continue decreasing. Hydraulic measurements revealed a drop of Lp_r during milder drought stress in the drought-resistant rootstock than in the drought-susceptible one coincident with lacunae formation in the former rootstock observed using micro-CT and in the same region where it was previously reported (Cuneo *et al.*, 2016). After re-watering, an increase of Lp_r was observed for the

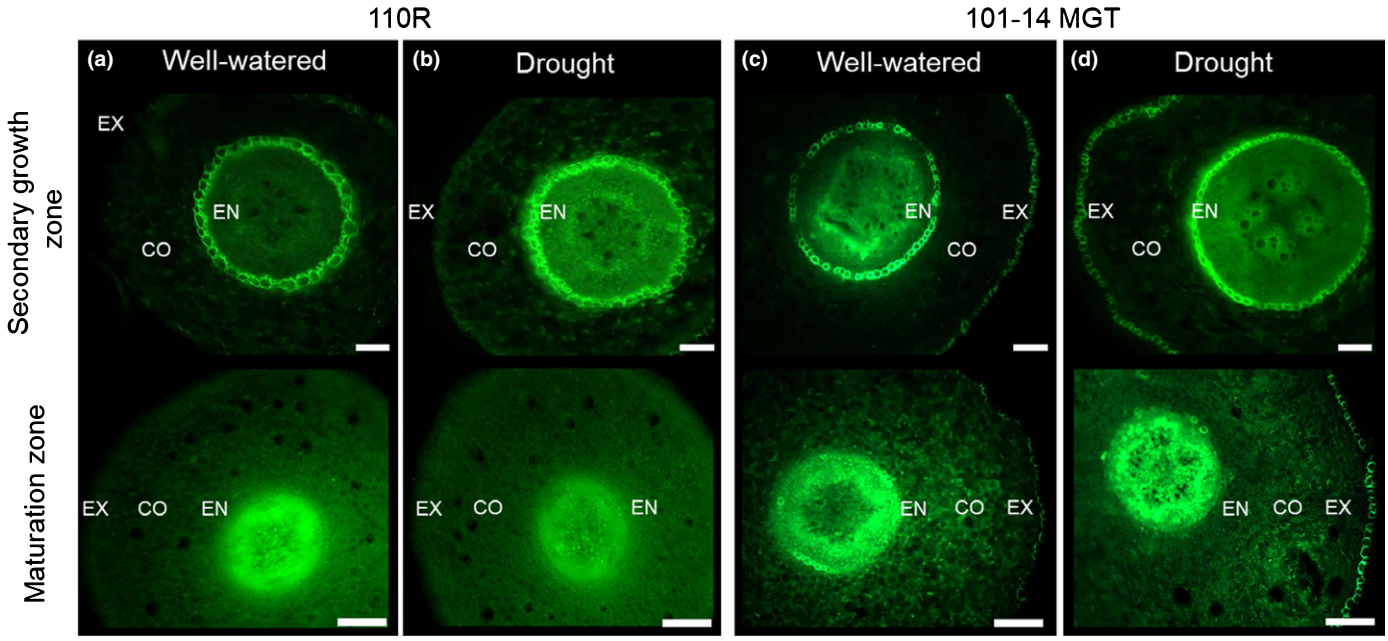

Fig. 4 Fluorescence microscopy showing anatomical traits of grapevine fine roots under well watered (i.e. *c.* −0.3 MPa Ψ_{stem}) and drought conditions (i.e. *c.* −1.0 MPa Ψ_{stem}) for 110R (a, b) and 101-14Mgt (c, d) rootstocks and in different developmental regions (i.e. maturation and secondary growth zone). Cross-sections stained with fluorol yellow 088 and imaged under fluorescent light (excitation filter, 450–490 nm; dichromatic mirror, 495 nm; and emission filter, 525 nm) showed more consistent and homogenous suberin deposition (appeared bright yellow) in 101-14Mgt (c, d). CO, cortex; EN, endodermis; EX, exodermis. Bars, 200 μm.

drought-resistant rootstock but not for the drought-susceptible one, coinciding with differences in re-establishment of root elongation rates between the rootstocks. Also, soil water status surrounding root tips differed between rootstocks as imaged with NR, which might be an indication of water depletion due to water uptake or water repellency due to hydrophobic mucilage in the rhizosphere of the drought-resistant rootstock (Ahmed *et al.*, 2015). The results presented here provide a detailed depiction of physiological and anatomical parameters related to drought responses in fine roots, and highlight the importance of rapid recovery of root elongation after re-watering as a key aspect in re-establishing root system functionality. Such a response would be beneficial in irrigated agricultural systems that experience similar degree of drying and rewetting of soil.

Fine root growth dynamics in response to abiotic and biotic stressors, seasonality and soil moisture at different depths have been extensively studied in the past using destructive and nondestructive techniques (Hendrick & Pregitzer, 1996; Tierney & Fahey, 2002; Comas *et al.*, 2005; Mainiero & Kazda, 2006; Lukac, 2012). Roots from different species have been reported to display either slow- or fast-growing patterns when transitioning from periods of low to high resource availability (Lambers & Poorter, 1992; Hodge, 2004). In general, plants that display fast-growing patterns have more morphological plasticity and are able to more rapidly utilize resources once they become available again (e.g. rain after drought; Crick & Grime, 1987; Hodge, 2004). In a previous study using rootstocks similar to those in the present study (1103P (*V. berlandieri* × *V. rupestris*) and 101-14Mgt) and minirhizotron tubes, Bauerle *et al.* (2008) found greater morphological plasticity and a larger shift in root diameter during low soil moisture in the drought tolerant rootstock 1103P. Consistent with this, both rootstocks in our study showed similar root elongation patterns during mild and severe drought stress, but fine roots in drought-resistant rootstock recovered root elongation after re-watering despite extensive lacunae formation. This pattern could be interpreted as a plastic response in the drought-resistant rootstock. The coincident re-establishment of Lp_r in the drought-resistant rootstock after 2 d of re-watering was not observed in the drought-susceptible one. We postulate that the rapid recovery of water uptake capacity after drought is linked to the capability of rootstocks to quickly resume root elongation (Fig. 7). We previously found that the xylem stays largely functional in grapevine fine roots even when lacunae have formed and Lp_r has dropped precipitously (Cuneo *et al.*, 2016); our current findings are consistent with this pattern for the two additional genotypes studied here (see images in Fig. 2). Retaining functionality of the xylem would permit rapid re-establishment of water absorption once a functional fine root cylinder had re-grown at the tip (Fig. 7). During drought, as cortical lacunae limit radial transport of mass and root elongation decreases, we hypothesize a shift of water uptake toward the root tip (Fig. 7), something that would be possible if xylem maturation occurs closer to the root tip during drought (i.e. similar to the drought-induced short roots in *Arabidopsis thaliana*, Couot-Gastelier & Vartanian, 1995). During water recovery (Fig. 7c), the newly formed root tissue contains a larger root meristematic-elongation zone compared with the root experiencing drought (Fig. 7b), similarly to the root before drought (Fig. 7a). In a previous study, Lp_r did not recover for 140Ru grapevine rootstock; however, plants were allowed to recover for only 24 h (see Cuneo *et al.*, 2016), which

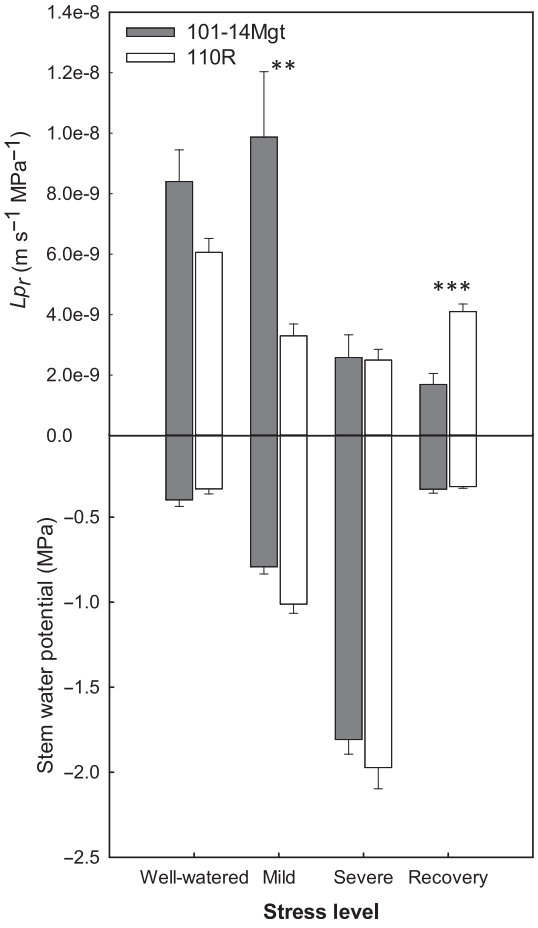

Fig. 5 Fine root hydraulic conductivity (Lp_r) and stem water potentials observed at different stress levels (i.e. Well watered, Mild, Severe and Recovery) for 101-14Mgt and 110R grapevine rootstocks. The Lp_r of 110R decreased abruptly during mild stress, while 101-14Mgt showed a decay in Lp_r at the severe stress level. During recovery (i.e. 48 h after re-watering), the Lp_r of 110R tended to increase, while the Lp_r of 101-14Mgt remained low and even continued to drop. Data are mean ± SE ($n = 10$). Asterisks indicate significant differences between rootstocks at each stress level as determined by *t*-test. **, $P < 0.01$; ***, $P < 0.001$.

was potentially not enough time to resume root elongation. By contrast, plants in this study were re-watered for 2 d before measuring Lp_r after recovery. Interestingly, Ψ_{stem} of both rootstocks did recover after re-watering, even for the drought-susceptible rootstock that did not display a recovery in fine root Lp_r. In this case, water uptake through permanent suberized coarse root might explain this recovery in Ψ_{stem} for the drought-susceptible rootstock. Previous studies have reported that water uptake through woody root portions (i.e. typically fourth order or higher roots) is possible (MacFall *et al.*, 1990, 1991; Cuneo *et al.*, 2018) and might be particularly relevant when the absorption pathways of fine roots are scarce or damaged (Green & Clothier, 1999; Dubrovsky & North, 2002; Cuneo *et al.*, 2016). Recently, direct evidence using micro-CT showed that water can enter woody roots through the lignified and suberized bark layer pointing to the water uptake potential of these roots (Cuneo *et al.*, 2018). Direct evidence using magnetic resonance imaging (MacFall *et al.*, 1990, 1991) and traditional hydraulic experiments (Queen, 1967; Chung & Kramer, 1975; Cuneo *et al.*, 2018) showed similar results, thus we feel this is a feasible explanation for the recovery in Ψ_{stem} in the drought-susceptible rootstock after re-watering. Also, here we observed water depletion : repellency patterns surrounding root tips after re-watering consistent with previous studies (water depletion, MacFall *et al.*, 1990, 1991; water repellency, Carminati *et al.*, 2010; Moradi *et al.*, 2012; Carminati, 2013; Ahmed *et al.*, 2015; Benard *et al.*, 2015; Zarebanadkouki *et al.*, 2018). This was observed specifically in the drought-resistant rootstock (Figs 6c, S5) and here we offer two hypotheses based on the observations: (1) water depletion that would confirm that the drought-resistant rootstock quickly resumes water uptake capacity after re-watering and (2) water repellency surrounding fine roots might help to hydraulically isolate the root tip from the drying soil, avoiding the risk of desiccation during drought. Recent results provide evidence that the formation of large gradients in water potential around the roots is prevented by stomata closure in Olives (Carminati *et al.*, 2020; Rodriguez-Dominguez & Brodribb, 2020). These results highlight the importance of accuracy when performing hydraulic experiment at the soil–root interface. Future experiments should consider different species, the type of root (i.e. pioneer or fibrous root) and root age (Carminati, 2013), and closely inspect the contents of the soil immediately adjacent to the roots.

Changes in fine root anatomy (i.e. cortical lacunae formation and differential deposition of suberin in exodermis and endodermis) during drought are important in understanding water uptake capacity. Formation of cortical lacunae has been reported in monocots (Esau, 1977; Stasovski & Peterson, 1991), desert succulents (North & Nobel, 1991, 1992, 1997), and recently in grapevine (Cuneo *et al.*, 2016). Suberization of the exodermis has similarly been observed in response to drought (Zimmermann & Steudle, 1998; Comas *et al.*, 2013). In a recent study of grapevines subjected to prolonged and repeated drying cycles and well watered treatments, 101-14Mgt roots suberized more rapidly and completely than 110R roots (Barrios-Masias *et al.*, 2015), consistent with our current results. A possible limitation of the fluorol yellow stain procedure used here is that it cannot detect suberin deposition associated with lignin in the Casparian strip (Naseer *et al.*, 2012), but the consistency with our results with those from the Barrios-Masias *et al.* (2015) study, which used a different staining procedure (i.e. berberine–aniline blue fluorescent stain) on the same rootstocks, lends credence to the current results. Lack of suberin deposition in fine roots of the drought-resistant rootstock might result in the maintenance of a biophysical connection with drying soil and, consequently, might explain cortical lacuna formation and subsequent drop in Lp_r reported here. This phenomenon was also observed in a previous study using the rootstock 140Ru (*V. berlandieri* × *V. rupestris*; Cuneo *et al.*, 2016). By contrast, the drought-susceptible rootstock deposited suberin more consistently in fine roots during drought. This suberin deposition might inhibit lacunae formation in the

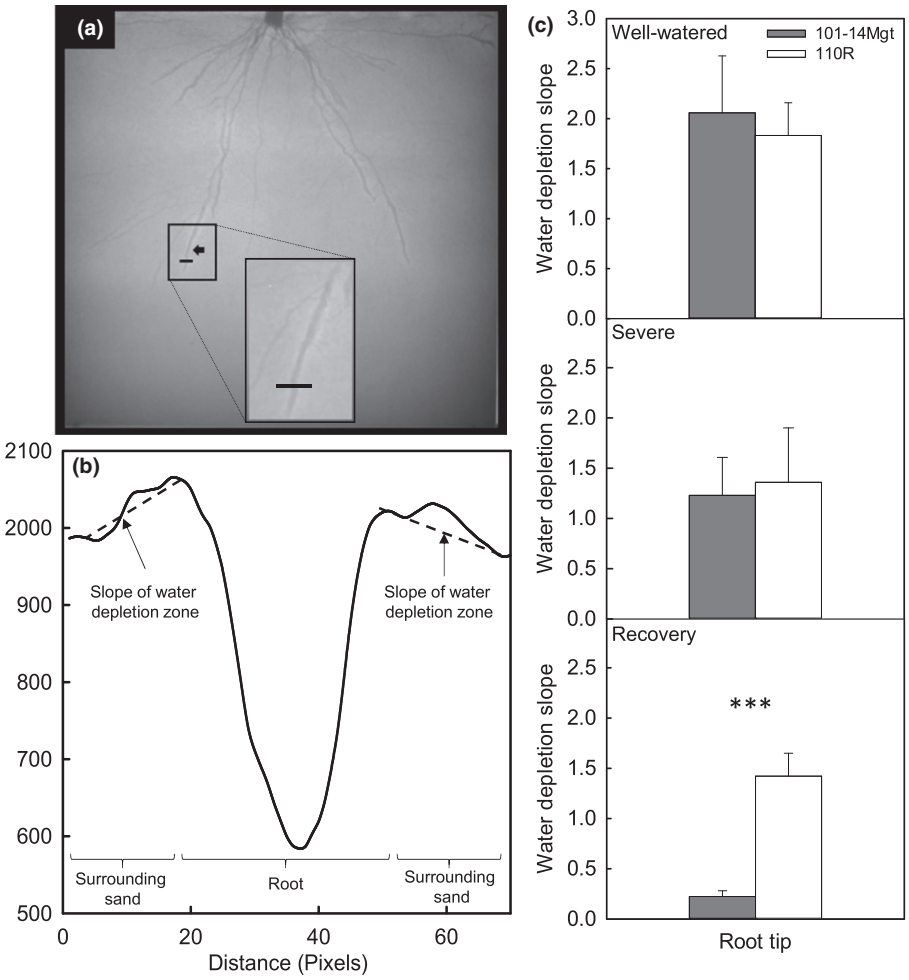

Fig. 6 (a) Representative neutron radiography (NR) scan showing water status surrounding grapevine roots tips (indicated by a black arrow and zoomed in the inset). (b) Plot profile corresponding to the black dashed line in the inset of (a). Gray values decrease with increasing soil moisture. A slope was calculated (dashed lines) using the gray pixel intensities the soil adjacent to the root tip (*c*. 4 mm from the surface of the root). (c) Water status slopes of the soil surrounding the root tip for 110R and 101-14Mgt for well watered, severe and recovery conditions. Data are mean ± SE ($n = 7$). Asterisks indicate significant differences between rootstocks at stress level as determined by *t*-test. ***, $P < 0.001$.

cortex of fine roots but might also result in reduced water uptake capacity upon re-watering. In this study, micro-CT scans targeted the maturation developmental region where cortical lacunae were previously found in the rootstock 140Ru (Cuneo *et al.*, 2016). However, future experiments should examine different developmental regions (e.g. root tip, maturation, and secondary growth zone) to elucidate how cortical lacunae formation is coupled with growth restoration in the root tip after re-watering, as well as how this affects water uptake capacity at the whole root system level.

The water uptake capacity of grapevine fine roots also depends on developmental anatomy and membrane permeability (Steudle, 2000; Gambetta *et al.*, 2012, 2013). Under nonstressed growing conditions, Gambetta *et al.* (2012) reported that the gene expression of several aquaporins (PIPs) was greater in 110R compared with 101-14Mgt, and this was associated with greater hydraulic conductivity in 110R (Gambetta *et al.*, 2012). Interestingly, PIP expression was greater in the root tip compared to mature root regions for 110R in two separate studies (Gambetta *et al.*, 2012, 2013), but the pattern was not found in 420A, a *V. berlandieri* × *V. riparia* low vigor and drought-susceptible rootstock. The concentration of aquaporin expression and activity in the root tips likely contribute to the drought-resistant rootstock ability to absorb water more effectively upon re-watering and thus enable roots to re-establish root elongation rapidly and enable depletion of water from the surrounding soil documented here. Similarly to cortical lacunae, future experiments should examine the expression and activity of aquaporins during drought and recovery in different root regions. Finally, plant hormone dynamics are known to affect root growth under favorable growing conditions (Cary *et al.*, 1995; Werner *et al.*, 2010), and likely play an important role in the root elongation responses of drought-resistant rootstock documented here, as well as in the developmental morphology of root systems over time.

Acknowledgements

IFC gratefully acknowledges the Fondecyt de Iniciación grant N°11180102 from Conicyt, Chile and DI-PUCV 37.0/2018. Also, this work was supported by USDA-ARS CRIS project 2032-21220-006-00D. The authors kindly thank D. Parkinson and A. MacDowell for their assistance at the Lawrence Berkeley National Laboratory Advanced Light Source (ALS) Beamline 8.3.2 microtomography facility. ALS is supported by the Director, Office of Science, Office of Basic Energy Science, of the US Department of Energy under contract no. DE-AC02-05CH11231. We also thank the California Grape Rootstock Improvement Commission for their generous funding support.

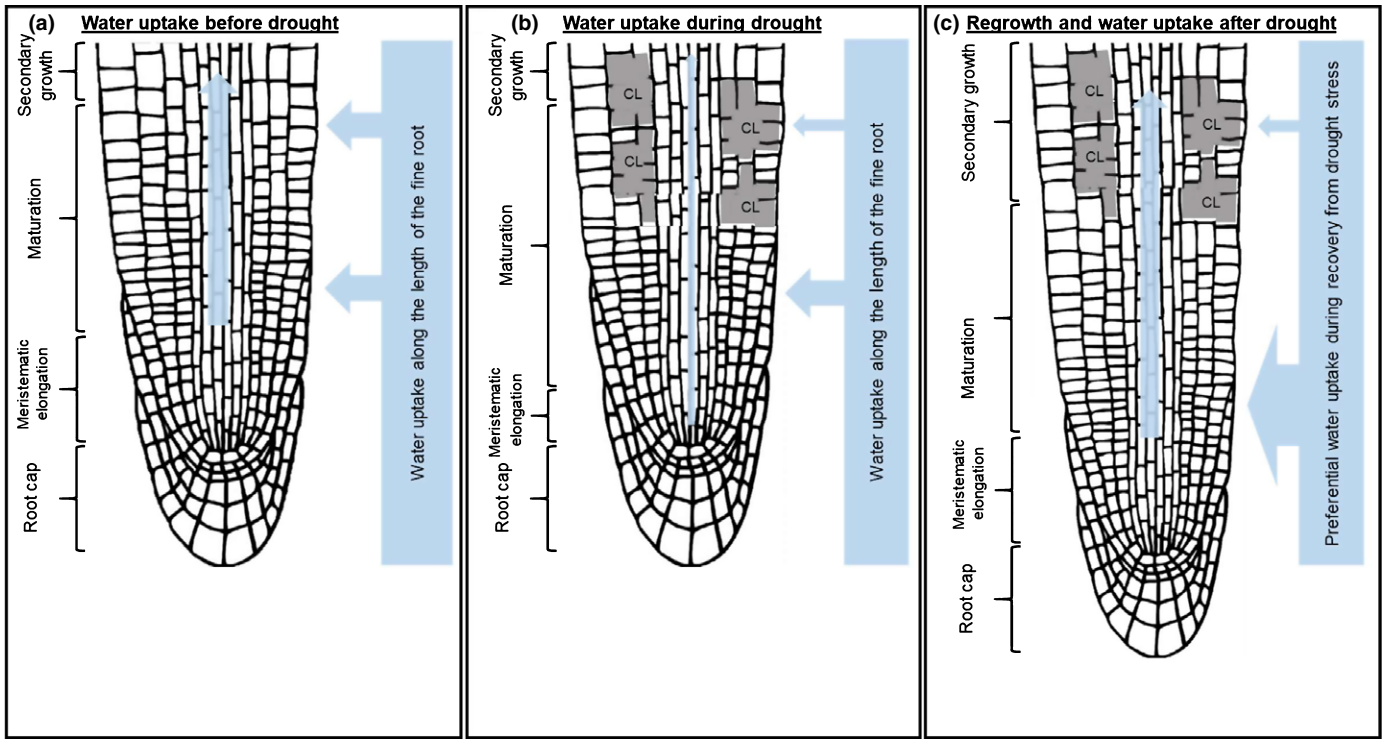

Fig. 7 Schematic illustration of a grapevine fine root showing: (a) water uptake along the length before drought stress, (b) water uptake limited by cortical lacunae formation during drought and water uptake shifting toward the root tip with a maturation developmental region getting closer to the tip, and (c) newly formed root tissue containing a larger root meristematic-elongation zone compared with (b) and similar to (a), with water uptake happening farther from the root tip. Hypothetically, the re-establishment of water uptake capacity in fine roots after a drought stress might be related to the capability of the root tip to keep growing after the stress, developing new root tissue and allowing the whole plant to re-establish the physiological function. In all panels, the root tip stays hydraulically isolated (Bret-Harte & Silk, 1994; Zwieniecki *et al.*, 2003). CL, cortical lacunae.

Author contributions

IFC and AJM designed the experiments. IFC and FB-M performed the NR imaging. IFC, TK and CR performed the micro-CT scanning; IFC, FB-M and CR performed the image analysis. IFC, CR and PL performed root hydraulics and microscopy essays; IFC and AJM wrote the initial draft of the article; JU, FB-M TK, CRB and MAW revised and edited the article; CRB and AJM obtained micro-CT beamtime.

ORCID

Craig R. Brodersen https://orcid.org/0000-0002-0924-2570
Italo F. Cuneo https://orcid.org/0000-0002-8092-0987
Andrew J. McElrone https://orcid.org/0000-0001-9466-4761

References

Ahmed M, Kroener E, Zarebanadkouki M, Kaestner A, Carminati A. 2015. Drying of mucilage causes water repellency in the rhizosphere of maize: measurements and modelling. *Plant and Soil* **407**: 164–171.

Aroca R, Porcel R, Ruiz-Lozano JM. 2011. Regulation of root water uptake under abiotic stress conditions. *Journal of Experimental Botany* **63**: 43–57.

Barrios-Masias FH, Knipfer TM, McElrone AJ. 2015. Differential responses of grapevine rootstocks to water stress are associated with adjustments in fine root hydraulic physiology and suberization. *Journal of Experimental Botany* **66**: 6069–6078.

Bauerle TL, Smart DR, Bauerle WL, Stockert C, Eissenstat DM. 2008. Root foraging in response to heterogeneous soil moisture in two grapevines that differ in potential growth rate. *New Phytologist* **179**: 857–866.

Benard P, Kroener E, Vontobel P, Kaestner A, Carminati A. 2015. Water percolation through the root–soil interface. *Advances in Water Resources* **95**: 190–198.

Bret-Harte MS, Silk WK. 1994. Nonvascular, symplasmic diffusion of sucrose cannot satisfy the carbon demands of growth in the primary root-tip of *Zea mays* L. *Plant Physiology* **105**: 19–33.

Brodersen CR, McElrone AJ, Choat B, Matthews MA, Shackel KA. 2010. The dynamics of embolism repair in xylem. *In vivo* visualizations using high-resolution computed tomography. *Plant Physiology* **154**: 1088–1095.

Brundrett MC, Kendrick B, Peterson CA. 1991. Efficient lipid staining in plant material with Sudan red 7B or Fluorol yellow 088 in polyethylene glycol–glycerol. *Biotechnic and Histochemistry* **66**: 111–116.

Carminati A. 2013. Rhizosphere wettability decreases with root age: a problem or a strategy to increase water uptake of young roots? *Frontiers in Plant Science* **4**: 298.

Carminati A, Ahmed MA, Zarebanadkoiki M, Cai G, Lovric G, Javaux M. 2020. Stomatal closure prevents the drop in soil water potential around roots. *New Phytologist*. doi: 10.1111/nph.16451.

Carminati A, Moradi A, Vetterlein D, Vontobel P, Lehmann E, Weller U, Vogel H-J, Oswald SE. 2010. Dynamics of soil water content in the rhizosphere. *Plant and Soil* **332**: 163–176.

Cary AJ, Liu W, Howell SH. 1995. Cytokinin action is coupled to ethylene in its effects on the inhibition of root and hypocotyl elongation in Arabidopsis thaliana seedlings. *Plant Physiology* **107**: 1075–1082.

Christensen L. 2003. Rootstock selection. In: Christensen PL, Dokoozlian KN, Walker AM, Wolpert JA, eds. *Wine grape varieties in California*. Oakland, CA, USA: University of California Agricultural and Natural Resources Publication, 12–15.

Chung HH, Kramer PJ. 1975. Absorption of water and ^{32}P through suberized and unsuberized roots of loblolly pine. *Canadian Journal of Forest Research* **5**: 229–235.

Comas LH, Andreson LJ, Dunst RM, Lakso AN, Eissenstat DM. 2005. Canopy and environmental control of root dynamics in a long-term study of Concord grape. *New Phytologist* **167**: 829–840.

Comas LH, Becker S, Cruz VMV, Byrne PF, Dierig DA. 2013. Root traits contributing to plant productivity under drought. *Frontiers in Plant Science* **4**: 442.

Couot-Gastelier J, Vartanian N. 1995. Drought-induced short roots in *Arabidopsis thaliana*: structural characteristics. *Botanica Acta* **108**: 407–413.

Crick JC, Grime JP. 1987. Morphological plasticity and mineral nutrient capture in two herbaceous species of contrasted ecology. *New Phytologist* **107**: 403–414.

Cuneo IF, Knipfer T, Brodersen CR, McElrone AJ. 2016. Mechanical failure of fine root cortical cells initiates plant hydraulic decline during drought. *Plant Physiology* **172**: 1669–1678.

Cuneo IF, Knipfer T, Mandal P, Brodersen C, McElrone A. 2018. Water uptake can occur through woody portions of roots and facilitates localized embolism repair in grapevine. *New Phytologist* **218**: 506–516.

Dubrovsky JG, North GB. 2002. Root structure and function in the Cactaceae. In: Nobel PS, ed. *Cactus biology and uses*. Berkeley, CA, USA: University of California Press, 41–56.

Esau K. 1977. *Anatomy of seed plants* (*2nd edn*). New York, NY, USA: Wiley.

Fox J, Weisberg S. 2011. *An {R} companion to applied regression, 2nd edn.* Thousand Oaks, CA, USA: Sage.

Gambetta GA, Fei J, Rost TL, Knipfer T, Matthews MA, Shackel KA, Walker MA, McElrone AJ. 2013. Water uptake along the length of grapevine fine roots: developmental anatomy, tissue-specific aquaporin expression, and pathways of water transport. *Plant Physiology* **163**: 1254–1265.

Gambetta GA, Manuck CM, Drucker ST, Shaghasi T, Fort K, Matthews MA, Walker MA, McElrone AJ. 2012. The relationship between root hydraulics and scion vigour across *Vitis* rootstocks: what role do root aquaporins play? *Journal of Experimental Botany* **63**: 6445–6455.

Geldner N. 2013. The endodermis. *Annual Review of Plant Biology* **64**: 531–558.

Green S, Clothier B. 1999. The root zone dynamics of water uptake by a mature apple tree. *Plant Soil* **206**: 61–77.

Hendrick RL, Pregitzer KS. 1996. Temporal and depth-related patterns of fine root dynamics in northern hardwood forests. *Journal of Ecology* **84**: 167–176.

Hodge A. 2004. The plastic plant: root responses to heterogeneous supplies of nutrients. *New Phytologist* **162**: 9–24.

Jackson RB, Sperry JS, Dawson TE. 2000. Root water uptake and transport: using physiological processes in global predictions. *Trends in Plant Science* **5**: 482–488.

Keller M. 2010. *The science of grapevines*. San Diego, CA, USA: Academic Press.

Knipfer T, Eustis AJ, Brodersen CR, Walker MA, McElrone AJ. 2015. Grapevine species from varied native habitats exhibit differences in embolism formation/repair associated with leaf gas exchange and root pressure. *Plant, Cell & Environment* **38**: 1503–1513.

Kramer PJ, Boyer JS. 1995. *Water relations of plant and soil*. San Diego, CA, USA: Academic Press.

Kramer PJ, Bullock HC. 1966. Seasonal variation in the proportions of suberized and unsuberized roots of trees in relation to the absorbed water. *American Journal of Botany* **53**: 200–204.

Lambers H, Poorter H. 1992. Inherent variation in growth rate between higher plants: a search for physiological causes and ecological consequences. *Advances in Ecological Research* **23**: 187–261.

Lukac M. 2012. *Fine root turnover. Measuring roots*. Berlin, Heidelberg, Germany: Springer.

MacFall JS, Johnson GA, Kramer PJ. 1990. Observation of a water-depletion region surrounding loblolly pine roots by magnetic resonance imaging. *Proceedings of the National Academy of Sciences, USA* **87**: 1203–1207.

MacFall JS, Johnson GA, Kramer PJ. 1991. Comparative water uptake by roots of different ages in seedlings of loblolly pine (*Pinus taeda* L.). *New Phytologist* **119**: 551–560.

Mainiero R, Kazda M. 2006. Depth-related fine root dynamics of *Fagus sylvatica* during exceptional drought. *Forest Ecology and Management* **237**: 135–142.

Maurel C, Verdoucq L, Luu DT, Santoni V. 2008. Plant aquaporins: membrane channels with multiple integrated functions. *Annual Review of Plant Biology* **59**: 595–624.

McCormack ML, Dickie IA, Eissenstat DM, Fahey TJ, Fernandez CW, Guo D, Helmisaari H-S, Hobbie EA, Iversen CM, Jackson RB *et al.* 2015. Redefining fine roots improves understanding of below-ground contributions to terrestrial biosphere processes. *New Phytologist* **207**: 505–518.

McElrone AJ, Choat B, Parkinson DY, MacDowell AA, Brodersen CR. 2013. Using high resolution computed tomography to visualize the three-dimensional structure and function of plant vasculature. *Journal of Visualized Experiments: JoVE* **74**: doi: 10.3791/50162.

Menon M, Robinson B, Oswald SE, Kaestner A, Abbaspour KC, Lehmann E, Schulin R. 2007. Visualization of root growth in heterogeneously contaminated soil using neutron radiography. *European Journal of Soil Science* **58**: 802–810.

Moradi AB, Carminati A, Lamparter A, Woche SK, Bachmann J, Vetterlein D, Vogel H-J, Sascha EO. 2012. Is the rhizosphere temporarily water repellent? *Vadose Zone Journal* **11**: doi: 10.2136/vzj2011.0120.

Naseer S, Lee Y, Lapierre C, Franke R, Nawrath C, Geldner N. 2012. Casparian strip diffusion barrier in Arabidopsis is made of a lignin polymer without suberin. *Proceedings of the National Academy of Sciences, USA* **109**: 10101–10106.

North GB, Nobel PS. 1991. Changes in hydraulic conductivity and anatomy caused by drying and rewetting roots of *Agave deserti* (Agavaceae). *American Journal of Botany* **78**: 906–905.

North GB, Nobel PS. 1992. Drought-induced changes in hydraulic conductivity and structure in roots of *Ferocactus acanthodes* and *Opuntia ficus-indica*. *New Phytologist* **120**: 9–19.

North GB, Nobel PS. 1997. Root-soil contact for the desert succulent *Agave deserti* in wet and drying soil. *New Phytologist* **135**: 21–29.

Pleinert H, Lehmann E. 1997. Determination of hydrogenous distributions by neutron transmission analysis. *Physica B: Condensed Matter* **234**: 1030–1032.

Pongrácz DP. 1983. *Rootstocks for grapevines*. Cape Town, South Africa: David Philip.

Queen WH. 1967. *Radial movement of water and ^{32}P through suberized and unsuberized roots of grape*. PhD thesis. Duke University, Durham, NC, USA.

R Core Team. 2016. *R: a language environment for statistical computing*. Vienna, Austria: R Foundation for Statistical Computing.

Richards JH, Caldwell MM. 1987. Hydraulic lift: substantial nocturnal water transport between soil layers by *Artemisia tridentata* roots. *Oecologia* **73**: 486–489.

Rodriguez-Dominguez CM, Brodribb TJ. 2020. Declining root water transport drives stomatal closure in olive under moderate water stress. *New Phytologist* **225**: 126–134.

Schindelin J, Arganda-Carreras I, Frise E, Kaynig V, Longair M, Pietzsch T, Preibisch S, Rueden C, Saalfeld S, Schmid B *et al.* 2012. Fiji: an open-source platform for biological-image analysis. *Nature Methods* **9**: 676–682.

Stasovski E, Peterson CA. 1991. The effects of drought and subsequent rehydration on the structure and vitality of *Zea mays* seedling roots. *Canadian Journal of Botany* **69**: 1170–1178.

Steudle E. 2000. Water uptake by roots: effects of water deficit. *Journal of Experimental Botany* **51**: 1531–1542.

Steudle E, Peterson CA. 1998. How does water get through roots? *Journal of Experimental Botany* **49**: 775–788.

Tierney GL, Fahey TJ. 2002. Fine root turnover in a northern hardwood forest: a direct comparison of the radiocarbon and minirhizotron methods. *Canadian Journal of Forest Research* **32**: 1692–1697.

van Dusschoten D, Metzner R, Kochs J, Postma JA, Pflugfelder D, Bühler J, Schurr U, Jahnke S. 2016. Quantitative 3D analysis of plant roots growing in soil using magnetic resonance imaging. *Plant Physiology* **170**: 11476–1188.

Vandeleur RK, Mayo G, Shelden MC, Gilliham M, Kaiser BN, Tyerman SD. 2009. The role of plasma membrane intrinsic protein aquaporins in water transport through roots: diurnal and drought stress responses reveal different strategies between isohydric and anisohydric cultivars of grapevine. *Plant Physiology* **149**: 445–460.

Werner T, Nehnevajova E, Kollmer I, Novak O, Strnad M, Kramer U, Schmulling T. 2010. Root-specific reduction of cytokinin causes enhanced

root growth, drought tolerance, and leaf mineral enrichment in arabidopsis and tobacco. *Plant Physiology* **22**: 3905–3920.

Zarebanadkouki M, Ahmed M, Hedwig C, Benard P, Kostka SJ, Kastner A, Carminati A. 2018. Rhizosphere hydrophobicity limits root water uptake after drying and subsequent rewetting. *Plant and Soil* **428**: 265–277.

Zimmermann HM, Steudle E. 1998. Apoplastic transport across young maize roots: effect of the exodermis. *Planta* **206**: 7–19.

Zimmermann MH. 1983. *Xylem structure and the ascent of sap*. Berlin, Germany: Springer.

Zwieniecki MA, Thompson MV, Holbroock NM. 2003. Understanding the hydraulics of porous pipes: tradeoffs between water uptake and root length utilization. *Journal of Plant Growth Regulation* **21**: 315–323.

Supporting Information

Additional Supporting Information may be found online in the Supporting Information section at the end of the article.

Fig. S1 Experimental set-up of neutron radiography at the McClellan Nuclear Research Center.

Fig. S2 Representative plot profiles of neutron radiographs across root tips of 110R and 101-14Mgt.

Fig. S3 Representative NR scans during the dry-down and recovery.

Fig. S4 Representative relationship between osmotic pressure and volumetric flow rate for 110R and 101-14Mgt fine roots.

Fig. S5 Pixel values of bulk soil near root tips, but outside the water depletion or water repellency zone.

Please note: Wiley Blackwell are not responsible for the content or functionality of any Supporting Information supplied by the authors. Any queries (other than missing material) should be directed to the *New Phytologist* Central Office.